

Research Article

Settlement Prediction of Foundation Pit Excavation Based on the GWO-ELM Model considering Different States of Influence

Qiao Shi-fan,¹ Tan Jun-kun,¹ Zhang Yong-gang ,² Wan Li-jun,³ Zhang Ming-fei,⁴ Tang Jun,⁵ and He Qing⁶

¹School of Civil Engineering, Central South University, Changsha 410083, China

²Key Laboratory of Geotechnical and Underground Engineering of Ministry of Education and Department of Geotechnical Engineering, Tongji University, Shanghai 200092, China

³Railway Engineering Research Institute, China Academy of Railway Science Co., Ltd., Beijing 12 100081, China

⁴Civil Engineering and Architecture Institute, Zhengzhou University of Aeronautics, Zhengzhou 450046, China

⁵College of Civil Engineering, Huaqiao University, Xiamen 361000, China

⁶School of Geotechnical Engineering, China University of Mining and Technology (Beijing), Beijing 100083, China

Correspondence should be addressed to Zhang Yong-gang; demonzhangy@tongji.edu.cn

Received 12 June 2020; Revised 13 November 2020; Accepted 13 January 2021; Published 27 January 2021

Academic Editor: Chunshun Zhang

Copyright © 2021 Qiao Shi-fan et al. This is an open access article distributed under the Creative Commons Attribution License, which permits unrestricted use, distribution, and reproduction in any medium, provided the original work is properly cited.

This paper proposes a novel grey wolf optimization-extreme learning machine model, namely, the GWO-ELM model, to train and predict the ground subsidence by combining the extreme learning machine with the grey wolf optimization algorithm. Taking an excavation project of a foundation pit of Kunming in China as an example, after analyzing the settlement monitoring data of cross sections JC55 and JC56, the representative monitoring sites JC55-2 and JC56-1 were selected as the training monitoring samples of the GWO-ELM model. And three kinds of GWO-ELM models such as considering the influence of time series, influence of settlement factors, and after optimization were established to predict the ground settlement near the foundation pit. The predictive results are that their average relative error and average absolute error are ranked from large to small as GWO-ELM model based on time series, GWO-ELM model based on settlement factors, and optimized GWO-ELM model for the three kinds of GWO-ELM models at monitoring points JC55-2 and JC56-1. Accordingly, the optimized GWO-ELM model has the strongest predictive ability.

1. Introduction

Responding to the demands of domestic social development, China constantly perfects the construction of urban underground space, and most of the foundation pit works involved are located in the central area of the city and belong to the deep foundation pit engineering. Due to the external conditions such as design and construction way, which can lead to settlement occurring in nearby area during the construction process, thus it will more or less affect nearby buildings, traffic road, and pipeline [1–3]. In order to reduce these negative impacts, it is necessary to choose scientific response policy and continuously promote the construction of engineering informatization; thereby, the settlement data around the project can be collected

timely, and the impact on nearby buildings and facilities can be analyzed. Thus, it can be seen that the key technology in them includes the prediction and study of the settlement in the vicinity area of the project.

Grey theory prediction method, complex theory method, and parameter accumulation method are the most common methods for predicting sedimentation [4–8]. The most popular used method is the grey theory prediction method which has a good effect on sequences including strong exponential laws and can explain the case of monotone transformation. However, it is difficult for this method to describe well when swinging. For example, the GM (1, 1) model is selected to predict the target of swing data, which will cause great errors [9, 10].

Different external environmental conditions have different impacts on the settlement of the area near the project; the final monitoring data is the result of the combined action of all the conditions and therefore has obvious nonlinear characteristics. So, in order to ensure the accuracy of the prediction results and as far as possible reduce the effects on nearby facilities, choosing good nonlinear mapping models is particularly important [4, 11]. Recently, some researchers chose to use neural network, BP neural network model [12–14], and support vector machine (SVM) model [15] to predict deformation of the supporting and bottom settlement, but almost did not involve the settlement in the nearby area during construction.

Although these intelligent algorithms have made some achievements [16–18], they also have some limitations. For example, BP neural network learning algorithm must set the network training parameters in the algorithm in the initialization, which usually leads to appearance of a case of locally optimal solution; SVM model has better prediction effect than neural network model, but the model itself has some defects such as difficulty in parameter selection. Extreme learning machine (ELM) is a new algorithm proposed in recent years [19, 20]; it is based on single hidden layer feedforward neural networks (SLFNs) and solved the problem that the number of hidden layers in the neural network is difficult to determine. Recent research regarding the application of ELM in geotechnical engineering is sufficiently applied, such as predicting compressive strength of lightweight foamed concrete using extreme learning machine model [21], prediction of shield tunneling-induced ground settlement using machine learning techniques [22], and landslide displacement prediction based on extreme learning machine [23]. Compared with traditional prediction models such as BP neural network and SVM, ELM learns faster, has good generalization ability, and produces the unique optimal solution. ELM can greatly improve the accuracy of classification by setting appropriate model parameters [24, 25]. In conventional methods, these parameters are mainly processed by grid search method, gradient descent method, particle swarm optimization (PSO) of metaheuristic search algorithm, and genetic algorithm (GA) of metaheuristic search algorithm [26, 27]. Grey wolf optimizer (GWO) [28] is a new metaheuristic algorithm that imitates the hunting behavior of wolf pack; GWO has the advantages of simple principle, few adjustment parameters, strong global search ability, and so on. In the study of combinatorial optimization problems, it has been proven to have significant advantages and has been widely applied in various fields [29–33].

In this paper, a new GWO-ELM model is established by combining the grey wolf algorithm with the extreme learning machine. Taking an excavation project of a foundation pit in Kunming as an example, after analyzing the settlement monitoring data of cross sections JC55 and JC56, the strong representative monitoring sites 55–2 and 56–1 were selected as the training monitoring samples of GWO-ELM model. And three kinds of GWO-ELM models such as considering the influence of time series and considering the influence of settlement factors and after optimization were

established to predict the ground settlement near the foundation pit.

2. Predictive Model of Ground Settlement of Foundation Pit Excavation Based on GWO-ELM

2.1. Extreme Learning Machine Model. ELM is a training method based on single hidden layer forward neural networks (SLFNs), which can calculate and analyze the output weight of the network. And this process only needs to set the threshold of hidden layer neurons to obtain the unique optimal solution and has a high learning speed. For N arbitrary and different samples (x_i, y_i) , where $x_i = [x_{i1}, x_{i2}, \dots, x_{im}]^T \in R^n$ and $y_i = [y_{i1}, y_{i2}, \dots, y_{im}]^T \in R^m$, there are L hidden layer neuron nodes, and the output of the standard feedforward neural network whose excitation function is $g(x)$ can be expressed as

$$f_L(x) = \sum_{i=1}^L \beta_i g(a_i \cdot x_i + b_i), \quad x_i \in R^n, \quad (1)$$

$$a_i \in R^n, \beta_i \in R^m,$$

where $a_i = [a_{i1}, a_{i2}, \dots, a_{im}]^T$ is the input weight from the input layer to the nodal point of the i th hidden layer; b_i is the threshold value of the i th neuron in the hidden layer; $\beta_i = [\beta_{i1}, \beta_{i2}, \dots, \beta_{im}]^T$ is the output weight of connecting the i th hidden layer node; $a_i \cdot x_i$ is the inner product of vector a_i and x_i ; and the excitation function $g(x)$ can be selected as “Sigmoid,” “RBF,” or “Sine” and so forth.

If the standard feedforward neural network with L hidden layer neurons and excitation function $g(x)$ can be with zero error to approach these N samples, then there exist a_i, b_i , and β_i resulting in

$$f_L(x) = \sum_{i=1}^L \beta_i g(a_i \cdot x_i + b_i) = y_i, \quad i = 1, 2, \dots, L. \quad (2)$$

Equation (2) can be simplified to

$$H\beta = Y, \quad (3)$$

where H is the output matrix of the neural network. In ELM, the output weight and threshold are randomly given, and the hidden layer matrix H becomes a definite matrix, which makes the training of feedforward neural network transform to a problem of finding the least square solution of the output weight matrix; the output weight matrix β is

$$\hat{\beta} = H^+ Y, \quad (4)$$

where H^+ represents the Moore–Penrose generalized inverse matrix of the hidden layer output matrix H , which can be obtained analytically by orthogonal projection or singular decomposition method and so on.

2.2. Grey Wolf Optimization. Grey wolf optimization (GWO) is a new swarm intelligent optimization algorithm

proposed by Mirjalili et al. which reproduces the hunting behavior of the grey wolf group by simulating the process of wolf pack tracking, surrounding, chasing, attacking prey, and such behaviors, so as to achieve the goal of optimization. GWO has the characteristics of simple principle, few adjustment parameters, strong global search ability, and so forth.

The searching optimal process of GWO is that a pack of grey wolves is randomly generated in the search space, according to the fitness high-low degree of α , β , and δ wolves of the grey wolf group to evaluate and locate the location of the prey. The rest of the individuals take this as the standard and calculate the distance between themselves and the prey to complete the prey capture and realize the process of searching optimal.

Definition 1. (social hierarchy). GWO model has a strict social class, which can be divided into α , β , δ , and ω wolves on the basis of the high and low level of the social class; the social rank in the algorithm is reflected in the fitness high-low degree.

Definition 2. (surrounding prey). In the process of wolf pack hunting, they need to surround the prey and determine the location of the prey; the mathematical equations of encirclement behavior are as follows:

$$\begin{aligned} D &= |C \cdot X_p(w) - X(w)|, \\ X(w+1) &= X_p(w) - \mu \cdot D, \\ C &= 2 \cdot r_1, \\ \mu &= 2a \cdot r_2 - a, \end{aligned} \quad (5)$$

where w is the current iteration number; $X_p(w)$ is the position vector of the prey in generation w ; $X(w)$ is the position vector of individual grey wolf in generation w ; $X(w+1)$ is the position vector of individual grey wolf in generation $w+1$; C is coefficient vector; r_1, r_2 belong to random vector, and its value range is $[0, 1]$; and μ is a vector of convergence; the value of a declines linearly from 2 to 0 during the iteration.

Definition 3. (hunting). The performance of wolf pack hunting process is hunting location information changed constantly. Specifically, in the iterative process, the algorithm saves the location of the best three wolves (α, β , and δ) currently obtained, and according to their information to update the location of other search unit wolves (ω) to obtain the optimal solution. Hunting behavior can be expressed as

$$\begin{aligned} D_k &= |C_i \cdot X_k(w) - X(w)|, \\ X_i &= X_k - \mu_i \cdot D_k, \\ X_p(w+1) &= \frac{X_1 + X_2 + X_3}{3}, \end{aligned} \quad (6)$$

where $k = \alpha, \beta, \gamma$; $i = 1, 2, 3$; and $X_p(w+1)$ is the position vector of the grey in generation $w+1$.

2.3. Forecasting Based on the GWO-ELM Model. This paper combines the grey wolf optimization algorithm with the extreme learning machine to train and predict the ground subsidence and proposes a grey wolf optimization-extreme learning machine model, namely, the GWO-ELM model.

The basic process is shown in Figure 1. Different states of influence and corresponding cumulative settlements are processed by the searching optimal process of GWO. If its suitability is verified, the relevant influencing factors are input into the ELM model, and finally the cumulative displacement prediction value is output.

3. The Construction of the GWO-ELM Model Based on Different States of Influence

3.1. Engineering Case Overview. In this paper, a foundation pit excavation project in Kunming is selected as a research case, which covers an area of 1.98 km². The ground subsidence measurement near the foundation pit adopts GPS monitoring technology, and the monitoring cross sections are divided into 110, which are named after JC1 to JC110 and set around the project.

The interval between the section and the section is 70–80 m, one cross-section has three monitoring points, and a total of 330 monitoring points are set. The research goal of this paper is a foundation pit in the engineering area, with a total area of 2465 m², a perimeter of 213 m, and a design depth of 7.6 m. The supporting method of the foundation pit is a curtain formed of arrangement of cement-soil mixing piles on the inside, and the formation stratum is composed of artificial fill, soft plastic clay, mucky clay, and slightly dense silty soil; the groundwater stable water level buried depth is 0.6–1.4 m. The settlement of the ground near the foundation pit is measured every seven days from June 1, 2019, until the end of November 30 and is monitored a total of 27 times. Figure 2 shows the measured values of the settlement of the cross sections JC55 and JC56. The data of the highly representative monitoring points of JC55-2 and JC56-1 are selected from them, and the GWO-ELM model considering different states of influence is constructed to predict ground settlement near the foundation pit.

3.2. Construction of the GWO-ELM Model Based on the Influence of Time Series. The first principle for parameter setting of GWO-ELM based on the influence of time series is to ensure accurate prediction accuracy, and on this basis, the model is simplified and the complexity is reduced to avoid the calculation speed being too slow. After the construction of the foundation pit starts, the settlement volume of the nearby ground will increase with the construction time. The reason for this phenomenon is that the construction of the foundation pit will cause the stress release of the nearby soil to change. Therefore, it is speculated that the construction time of the foundation pit has a certain correlation with the ground settlement near the foundation pit, and through the universal law of past data to predict settlement volume.

In this paper, the settlement volume data of a certain measurement are represented by the sequence $W(1), W(2),$

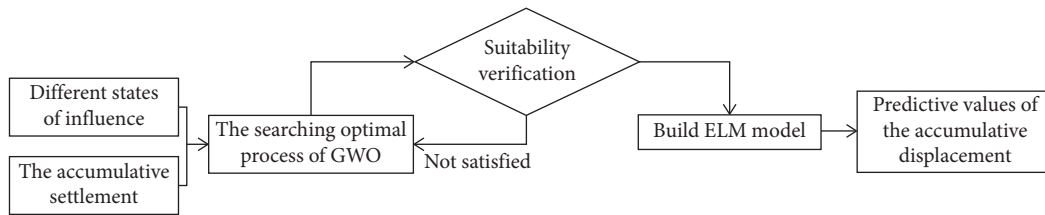


FIGURE 1: Flowchart of predicting ground settlement of foundation pit excavation with GWO-ELM model.

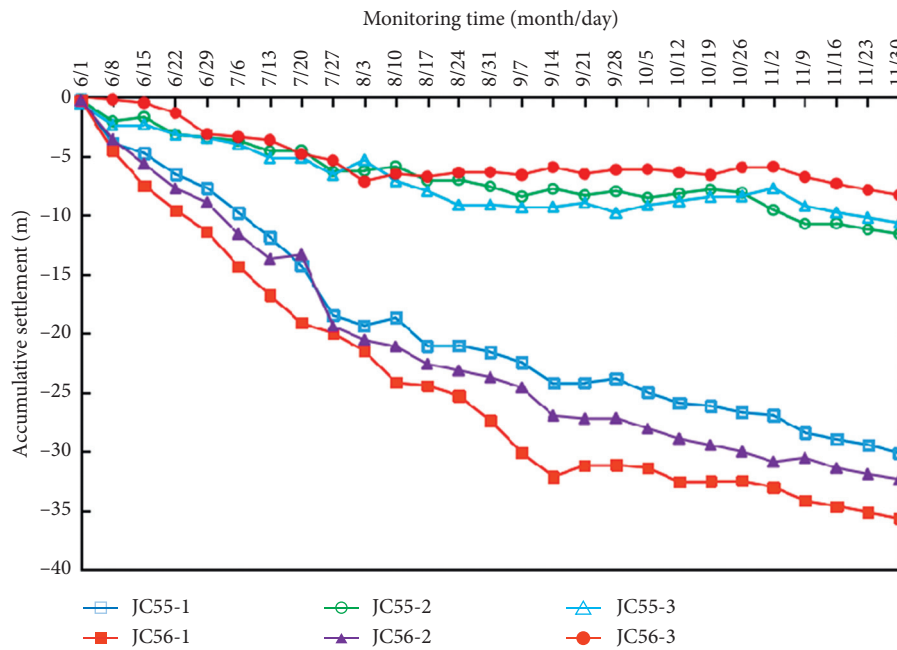


FIGURE 2: Cumulative settlement of different monitoring points.

..., $W(n)$, and the measurement data after this time are represented by $W(n+1)$, $W(n+2)$, Select m measurement data as the input layer of the model in $W(1)$, $W(2)$, ..., $W(n)$, thereby forming a training sample, and at the same time, the $m+1$ measurement value $W(m+1)$ was set to the model output value, constitute a total of $n-m$ groups of training samples and prediction target values, and start training; after that, $W(n-m+1)$, $W(n-m+2)$, ..., $W(n)$ input into the trained GWO-ELM model, the predicted value of $W(n+1)$ can be calculated out (Figure 3).

When the number of the input layer nodes is set to 12, the amount of computation generated by the GWO-ELM neural network model considering the influence of time series is not large, and at the same time, it can ensure better accuracy of settlement prediction. To a great extent, the model performance was affected by the quantity of hidden layers and the number of nodes in the initial structure of the model. After comparing the training time and operation result of different nodes between the single hidden layer and the two hidden layers, it is found that the double hidden layer does the prediction accuracy and meets the requirements; meanwhile, the training time required is shorter. And the number of nodes with the best performance should be set to 10. In summary, the GWO-ELM model based on the influence of time series finally adopts the 12-10-2 structure.

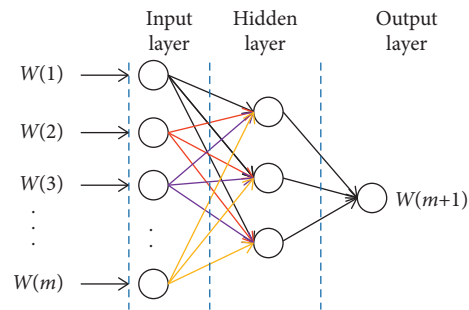


FIGURE 3: GWO-ELM model structure based on the influence of time series.

3.3. Construction of the GWO-ELM Model Based on the Influence of Settlement Factors. There are many factors that affect the ground settlement near the foundation pit, and the influence degree of each factor on the settlement is unsure (Figure 4). It is very difficult for the previous prediction methods to accurately predict the amount of settlement based on these influencing factors. And the advantage of the GWO-ELM model based on the influence of settlement factors is that it has a better nonlinear fitting function, so as to obtain a predicted value with higher accuracy.

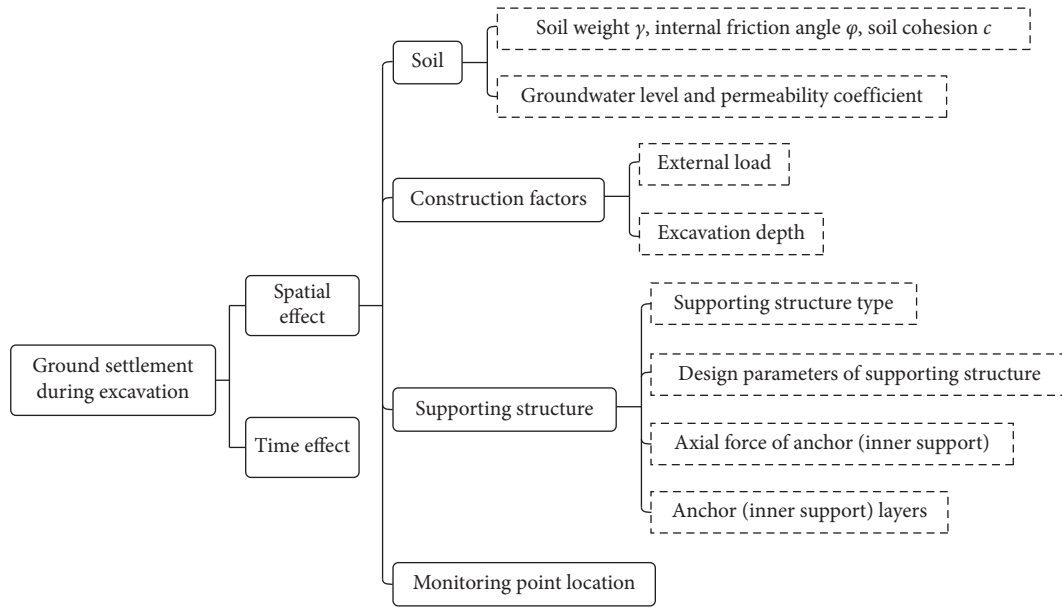


FIGURE 4: Influencing factors of ground settlement near the foundation pit.

The input layer of the GWO-ELM model based on the influence of settlement factors contains a total of 6 influencing factors (as shown in Figure 5). These factors are used as the input layer of the model, and the actual measured value of the formation settlement is the output layer of the model. The number of nodes in the hidden layer of the model is consistent with the above model, and the structure of the GWO-ELM model based on the influence of settlement factors is 6-10-2 structure.

In Figure 5, γ is soil weight; φ is internal friction angle; c is soil cohesion; k is weighted average of formation permeability coefficient; h is deep excavation depth; d is the distance between the monitoring point and the groove side of the foundation pit.

3.4. Construction of the Optimized GWO-ELM Model Based on Time Series and Settlement Factors. By optimizing the GWO-ELM model based on the influence of settlement factors, adding the previous settlement data in the input layer, so that the input value includes the formation parameters near the foundation pit, construction conditions, and real-time settlement monitoring data; thus, the design of model is optimized. As shown in Figure 6, compared with the GWO-ELM model only considering the influence of sedimentation, the GWO-ELM model after optimization added the parameters of three sedimentation time nodes before the prediction target, which were represented by z_1 , z_2 , and z_3 , respectively. The model structure after optimization adopted the 9-10-2 structure.

4. Analysis of Settlement Prediction Results of the GWO-ELM Model Based on Different States of Influence

In this paper, the settlement monitoring points JC55-2 and JC56-1 are selected for GWO-ELM model learning. Eighteen settlement datasets from June 1, 2019, to October 5, 2019, were used as training samples for training (Figure 7). And

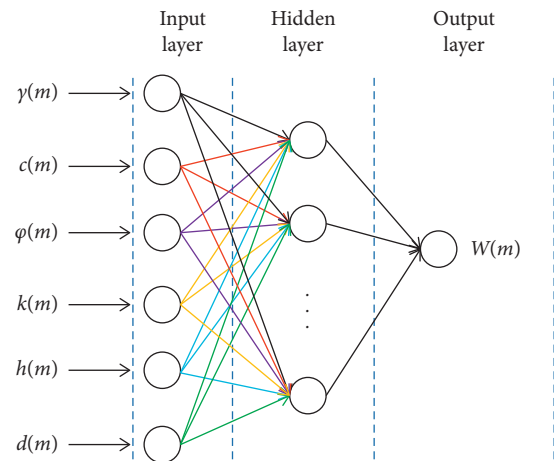


FIGURE 5: GWO-ELM model structure based on the influence of settlement factors.

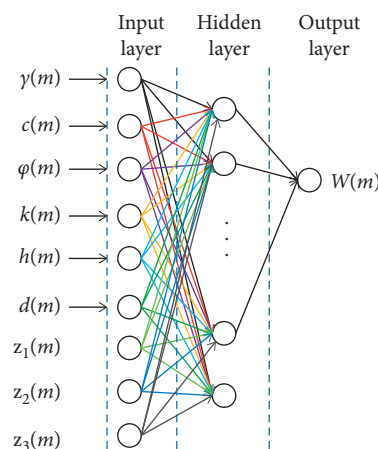


FIGURE 6: The optimized GWO-ELM model structure.

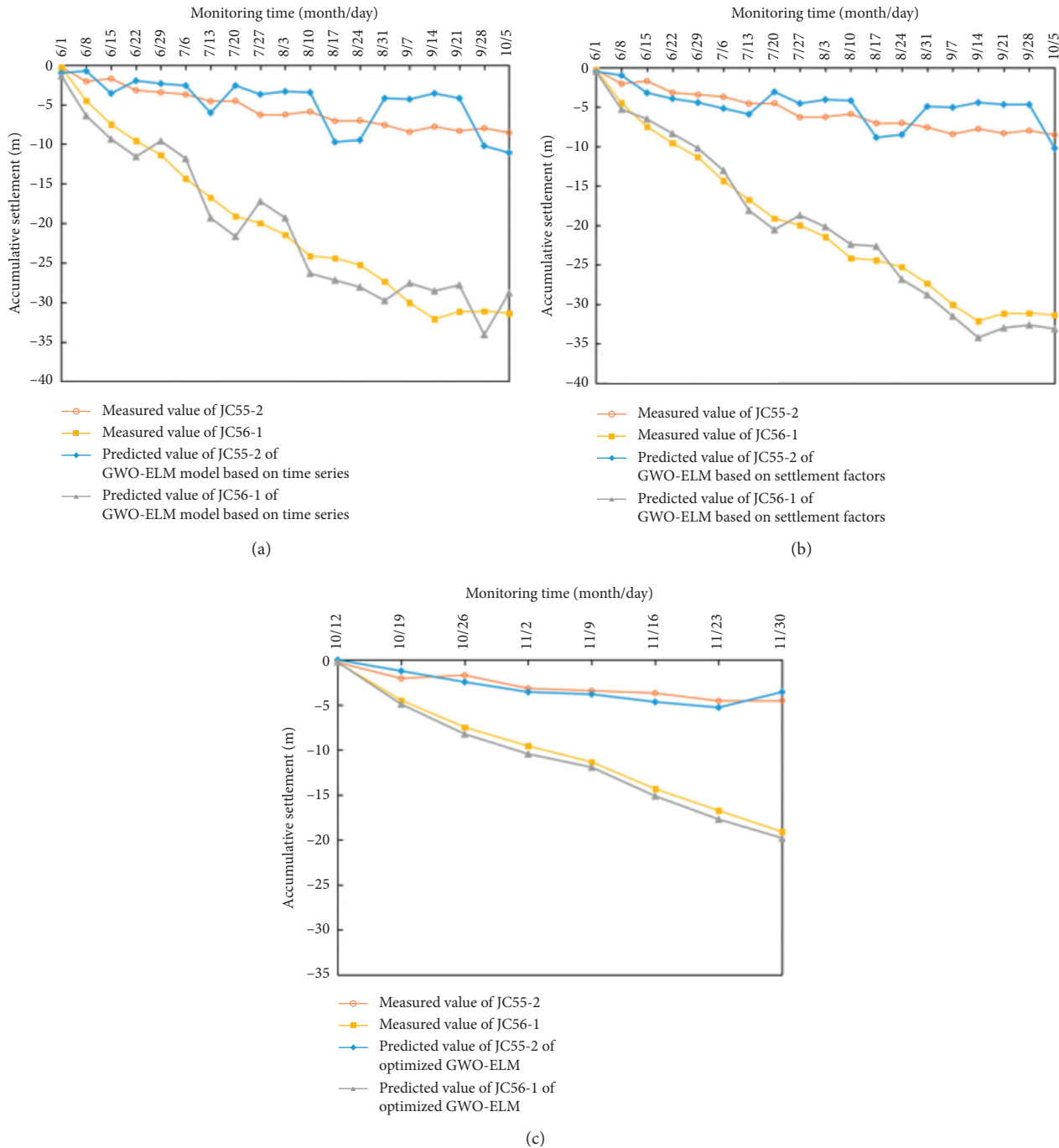


FIGURE 7: Comparison of GWO-ELM model prediction results based on different influence states.

nine settlement datasets from October 12, 2019, to November 30, 2019, were used as test samples. The following are the prediction results of the GWO-ELM model based on different states of influence.

4.1. Settlement Results Prediction Analysis of the GWO-ELM Model Based on Time Series. It can be seen from Figure 8 and Table 1, considering the influence of time series, the prediction results of the GWO-ELM model for the settlement monitoring sites JC55-2 and JC56-1 are relatively

close to the actual monitoring settlement results. At the monitoring point JC55-2, the absolute error range of the actual accumulative settlement and the predicted value is within 0.98 m–4.70 m, and the average absolute error is 2.42 m; the relative error range is within 8.79%–43.80%, and the average relative error value is 25.40%. At the monitoring point JC56-1, the absolute error range of the actual accumulative settlement and the predicted value is within 2.45 m–3.39 m, and the average absolute error is 2.84 m; the relative error range is within 7.13%–9.52%, and the average relative error value is 8.41%.

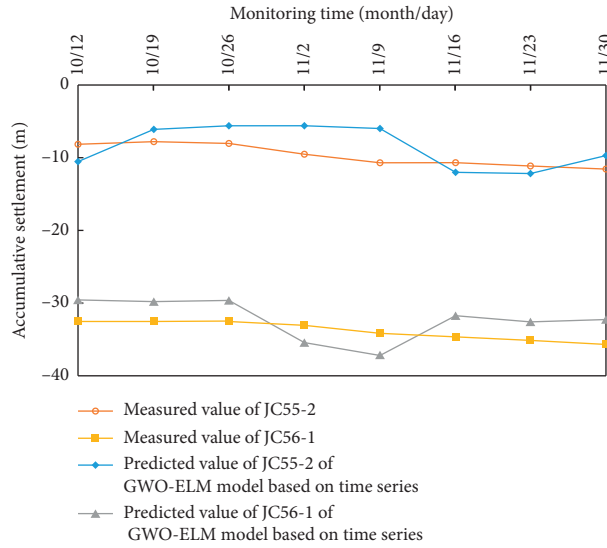


FIGURE 8: Settlement results prediction of GWO-ELM model based on time series.

TABLE 1: Settlement results prediction of GWO-ELM model based on time series.

Time	Accumulative settlement of JC55-2	Accumulative settlement of JC56-1	Predictive results of JC55-2	Predictive results of JC56-1	Absolute error of JC55-2 (m)	Absolute error of JC56-1 (m)	Relative error of JC55-2 (%)	Relative error of JC56-1 (%)
10/12	-8.18	-32.54	-10.58	-29.54	2.41	3.00	29.41	9.22
10/19	-7.83	-32.49	-6.15	-29.78	1.68	2.71	21.40	8.33
10/26	-8.09	-32.44	-5.66	-29.66	2.43	2.77	30.05	8.55
11/2	-9.55	-32.99	-5.66	-35.45	3.89	2.45	40.74	7.43
11/9	-10.73	-34.12	-6.03	-37.17	4.70	3.04	43.80	8.92
11/16	-10.69	-34.59	-12.06	-31.75	1.37	2.84	12.85	8.20
11/23	-11.20	-35.12	-12.18	-32.62	0.98	2.50	8.79	7.13
11/30	-11.60	-35.64	-9.72	-32.25	1.88	3.39	16.18	9.52
Min	—	—	—	—	0.98	2.45	8.79	7.13
Max	—	—	—	—	4.70	3.39	43.80	9.52
Mean	—	—	—	—	2.42	2.84	25.40	8.41

4.2. Settlement Results Prediction Analysis of the GWO-ELM Model Based on Settlement Factors. As can be seen from Figure 9 and Table 2, considering the influence of settlement factors, the prediction results of the GWO-ELM model for the settlement monitoring points JC55-2 and JC56-1 are close to the actual monitoring results. At the monitoring point JC55-2, the absolute error range of the actual cumulative settlement and the predicted value is within 0.95 m–1.62 m, and the average absolute error is 1.34 m; the relative error range is within 8.22%–19.47%, and the average relative error value is 14.26%. At the monitoring point JC56-1, the absolute error range of the actual cumulative settlement and the predicted value is within 1.30 m–1.85 m, and the average absolute error is 1.64 m; the relative error range is within 4.00%–5.44%, and the average relative error is 4.86%. Compared with the GWO-ELM model that only considers the influence of time series, the prediction accuracy of this model is higher.

4.3. Settlement Results Prediction Analysis of the Optimized GWO-ELM Model. It can be seen from Figure 10 and Table 3

that the prediction results of the optimized GWO-ELM model for settlement monitoring points JC55-2 and JC56-1 are very close to the actual monitoring results. At the monitoring point JC55-2, the absolute error range of the actual accumulative settlement and the predicted value is within 0.35 m–0.65 m, and the average absolute error is 0.47 m; the relative error range is within 3.22%–7.97%, and the average relative error value is 4.98%. At the monitoring point JC56-1, the absolute error range of the actual cumulative settlement and the predicted value is within 0.56 m–0.74 m, and the average absolute error is 0.66 m; the relative error range is within 1.72%–2.28%, and the average relative error value is 1.95%. Compared with the GWO-ELM model that only considers the influence of settlement, the prediction accuracy of this model is higher.

4.4. Comparison of GWO-ELM Model Prediction Errors of Different Influence States. As shown in Figures 11(a) and 11(b), for the three GWO-ELM models at monitoring points JC55-2 and JC56-1, their average relative error and average

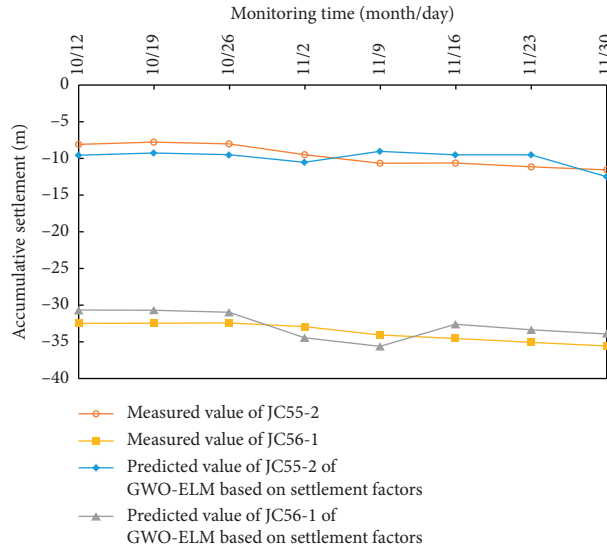


FIGURE 9: Settlement results prediction of GWO-ELM model based on time series.

TABLE 2: Settlement results prediction of GWO-ELM model based on time series.

Time	Accumulative settlement of JC55-2	Accumulative settlement of JC56-1	Predictive results of JC55-2	Predictive results of JC56-1	Absolute error of JC55-2 (m)	Absolute error of JC56-1 (m)	Relative error of JC55-2 (%)	Relative error of JC56-1 (%)
10/12	-8.18	-32.54	-9.60	-30.77	1.42	1.77	17.37	5.44
10/19	-7.83	-32.49	-9.35	-30.77	1.52	1.72	19.47	5.30
10/26	-8.09	-32.44	-9.60	-31.14	1.51	1.30	18.62	4.00
11/2	-9.55	-32.99	-10.58	-34.58	1.03	1.59	10.78	4.82
11/9	-10.73	-34.12	-9.11	-35.69	1.62	1.57	15.13	4.59
11/16	-10.69	-34.59	-9.60	-32.74	1.09	1.85	10.18	5.35
11/23	-11.20	-35.12	-9.60	-33.48	1.60	1.64	14.29	4.68
11/30	-11.60	-35.64	-12.55	-33.97	0.95	1.67	8.22	4.69
Min	—	—	—	—	0.95	1.30	8.22	4.00
Max	—	—	—	—	1.62	1.85	19.47	5.44
Mean	—	—	—	—	1.34	1.64	14.26	4.86

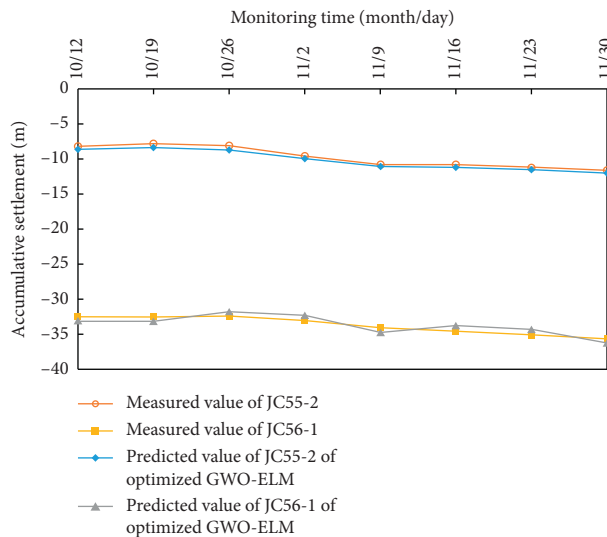


FIGURE 10: Settlement results prediction of the optimized GWO-ELM model.

TABLE 3: Settlement results prediction of the optimized GWO-ELM model.

Time	Accumulative settlement of JC55-2	Accumulative settlement of JC56-1	Predictive results of JC55-2	Predictive results of JC56-1	Absolute error of JC55-2 (m)	Absolute error of JC56-1 (m)	Relative error of JC55-2 (%)	Relative error of JC56-1 (%)
10/12	-8.18	-32.54	-8.62	-33.11	0.44	0.57	5.33	1.75
10/19	-7.83	-32.49	-8.37	-33.23	0.54	0.74	6.89	2.28
10/26	-8.09	-32.44	-8.74	-31.88	0.65	0.56	7.97	1.72
11/2	-9.55	-32.99	-9.97	-32.37	0.41	0.62	4.34	1.89
11/9	-10.73	-34.12	-11.08	-34.83	0.35	0.71	3.22	2.07
11/16	-10.69	-34.59	-11.20	-33.85	0.51	0.74	4.79	2.15
11/23	-11.20	-35.12	-11.57	-34.46	0.37	0.66	3.30	1.87
11/30	-11.60	-35.64	-12.06	-36.31	0.46	0.67	3.98	1.87
Min	—	—	—	—	0.35	0.56	3.22	1.72
Max	—	—	—	—	0.65	0.74	7.97	2.28
Mean	—	—	—	—	0.47	0.66	4.98	1.95

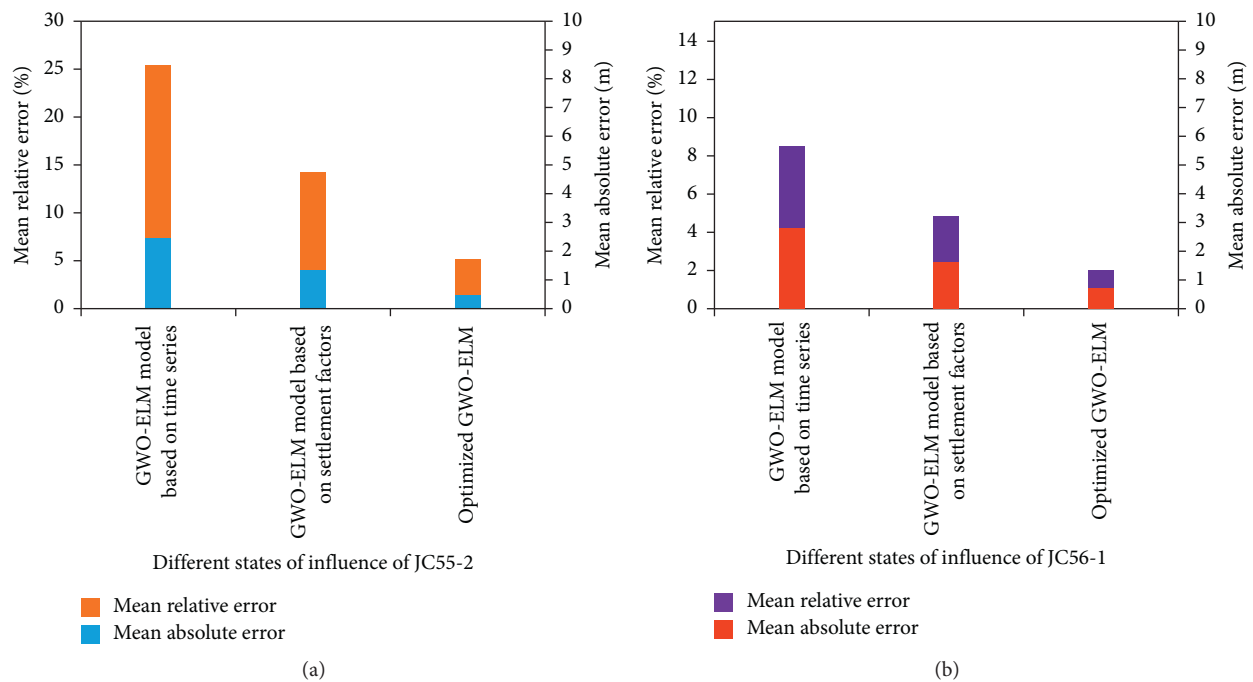


FIGURE 11: Comparison of GWO-ELM model prediction errors of different influence states.

absolute error are ranked from large to small as GWO-ELM model based on time series, GWO-ELM model based on settlement factors, and optimized GWO-ELM model. Accordingly, the optimized GWO-ELM model has the strongest predictive ability.

Through the comparison of different models, it is found that the more factors considered, the higher the prediction accuracy of the model in the prediction process. The optimized GWO-ELM model is more suitable for the settlement prediction of foundation pit excavation.

Although the optimized model in this paper predicts settlement displacement with high accuracy, the amount of data collected by the model is still relatively small. If you want to apply the model to other projects, you need to improve the applicability of the model. In order to improve

application ability, one needs to learn settlement data in other engineering projects.

5. Conclusion

- (1) This paper combines the grey wolf optimization algorithm with the extreme learning machine to train and predict the ground subsidence and proposes a novel grey wolf optimization-extreme learning machine model, namely, the GWO-ELM model. Taking an excavation project of a foundation pit in Kunming as an example, after analyzing the settlement monitoring data of cross sections JC55 and JC56, the representative monitoring sites JC55-2 and JC56-1 were selected as the training

monitoring samples of the GWO-ELM model. And three kinds of GWO-ELM models such as considering the influence of time series and considering the influence of settlement factors and after optimization were established to predict the ground settlement near the foundation pit.

- (2) After learning the monitoring data with the GWO-ELM model considering the influence of time series, it is found that, at settlement monitoring points JC55-2 and JC56-1, the average absolute error between the actual accumulated settlement and the predicted value was, respectively, in 2.42 m and 2.84 m, and the average relative error was, respectively, in 25.40% and 8.40%.
- (3) The average absolute error between the actual cumulative settlement and the predicted value at the settlement monitoring points JC55-2 and JC56-1 of the GWO-ELM model considering the settlement factor is 1.34 m and 1.64 m, respectively, and the average relative error values are 14.26% and 4.86%. Compared with the GWO-ELM model which only considers the influence of time series, this model can better predict the settlement of the ground near the excavation of the foundation pit.
- (4) At the settlement monitoring points JC55-2 and JC56-1 of the optimized GWO-ELM model, the average absolute error between the actual cumulative settlement and the predicted value is, respectively, in 0.47 m and 0.66 m, and the average relative error is, respectively, in 4.98% and 1.95%. Compared with the previous two models, the prediction results of the monitoring points JC55-2 and JC56-1 are closer to the actual monitoring results, and the prediction effect is better.

Data Availability

The data used to support the findings of the study are available from the corresponding author upon request.

Conflicts of Interest

The authors declare that they have no conflicts of interest.

Authors' Contributions

Qiao Shi-fan developed methodology; Zhang Mingfei contributed to software; Tan Junkun and Wang Weiting validated the study; Zhang Yonggang and Tang Jun wrote the original manuscript; Qiao Shi-fan, Tan Junkun, Zhang Yonggang, and Chen Fei reviewed and edited the article.

Acknowledgments

The authors appreciate the financial support provided by National Natural Science Foundation of China under Grant no. 41902266.

References

- [1] L. Liu, Z. Li, G. Cai, X. Liu, and S. Yan, "Humidity field characteristics in road embankment constructed with recycled construction wastes," *Journal of Cleaner Production*, vol. 259, Article ID 120977, 2020.
- [2] C. Xu, D. Yue, and C. Deng, "Hybrid GA/SIMPLS as alternative regression model in dam deformation analysis," *Engineering Applications of Artificial Intelligence*, vol. 25, no. 3, pp. 468–475, 2012.
- [3] N. Q. Zhou, P. A. Vermeer, R. X. Lou, Y. Q. Tang, and S. M. Jiang, "Numerical simulation of deep foundation pit dewatering and optimization of controlling land subsidence," *Engineering Geology*, vol. 114, no. 3-4, pp. 251–260, 2010.
- [4] G. Li, C. Wen, W. X. Zheng, and Y. Chen, "Identification of a class of nonlinear autoregressive models with exogenous inputs based on kernel machines," *IEEE Transactions on Signal Processing*, vol. 59, no. 5, pp. 2146–2159, 2011.
- [5] T. Matsubara and J. Morimoto, "Bilinear Modeling of EMG Signals to Extract User-Independent Features for Multiuser Myoelectric Interface," *IEEE Transactions on Biomedical Engineering*, vol. 60, no. 8, pp. 2205–2213, 2013.
- [6] A. Wiesel, O. Bibi, and A. Globerson, "Time Varying Autoregressive Moving Average Models for Covariance Estimation," *IEEE Transactions on Signal Processing*, vol. 61, no. 11, pp. 2791–2801, 2013.
- [7] Y. Zhang, S. Zhu, W. Zhang, and H. Liu, "Analysis of deformation characteristics and stability mechanisms of typical landslide mass based on the field monitoring in the Three Gorges Reservoir, China," *Journal of Earth System Science*, vol. 1289, no. 1, 2019.
- [8] Y. Zhang, S. Zhu, J. Tan, L. Li, and X. Yin, "The influence of water level fluctuation on the stability of landslide in the Three Gorges Reservoir," *Arabian Journal of Geosciences*, vol. 13845 pages, 2020.
- [9] Q. G. Feng, C. B. Zhou, Z. F. Fu, and G. C. Zhang, "Grey fuzzy variable decisionmaking model of supporting schemes for foundation pit," *Rock and Soil Mechanics*, vol. 31, no. 7, pp. 2226–2231, 2010.
- [10] R. Liu and X.-L. Li, "Deformation monitoring and forecasting model study based on grey system theory," *Advances in Soft Computing*, vol. 2, pp. 555–564, 2009.
- [11] Y. Zhang, Z. Zhang, S. Xue, R. Wang, and M. Xiao, "Stability analysis of a typical landslide mass in the Three Gorges Reservoir under varying reservoir water levels," *Environmental Earth Sciences*, vol. 79, no. 1, 2020.
- [12] A. Ismail and D.-S. Jeng, "Modelling load-settlement behaviour of piles using high-order neural network (HON-PILE model)," *Engineering Applications of Artificial Intelligence*, vol. 24, no. 5, pp. 813–821, 2011.
- [13] S. S. Leu and H. C. Lo, "Neural-network-based regression model of ground surface settlement induced by deep excavation," *Automation in Construction*, vol. 13, no. 3, pp. 279–289, 2004.
- [14] G. Zhang, X. Xiang, and H. Tang, "Time series prediction of chimney foundation settlement by neural networks," *International Journal of Geomechanics*, vol. 11, no. 3, pp. 154–158, 2011.
- [15] Y. Zhou, W. Su, L. Ding, H. Luo, and P. E. D. Love, "Predicting safety risks in deep foundation pits in subway infrastructure projects: support vector machine approach," *Journal of Computing in Civil Engineering*, vol. 31, no. 5, pp. 040170521–0401705214, 2017.

- [16] Y.-G. Zhang, J. Tang, Z.-Y. He, J. Tan, and C. Li, "A novel displacement prediction method using gated recurrent unit model with time series analysis in the Erdaohe landslide," *Natural Hazards*, vol. 105, no. 1, p. 783, 2020.
- [17] Y.-G. Zhang, J. Tang, R.-P. Liao et al., "Application of an enhanced BP neural network model with water cycle algorithm on landslide prediction," *Stochastic Environmental Research and Risk Assessment*, 2020.
- [18] Y. Zhang and L. Yang, "A novel dynamic predictive method of water inrush from coal floor based on gated recurrent unit model," *Natural Hazards*, 2020.
- [19] G.-B. Huang, D. H. Wang, and Y. Lan, "Extreme learning machines: a survey," *International Journal of Machine Learning and Cybernetics*, vol. 2, no. 2, pp. 107–122, 2011.
- [20] M. Xia, Y. Zhang, L. Weng, and X. Le, "Fashion retailing forecasting based on extreme learning machine with adaptive metrics of inputs," *Knowledge Based Systems*, vol. 36, pp. 253–259, 2020.
- [21] M. Shariati, M. S. Mafipour, B. Ghahremani et al., "A novel hybrid extreme learning machine-grey wolf optimizer (ELM-GWO) model to predict compressive strength of concrete with partial replacements for cement," *Engineering with Computers*, 2020.
- [22] R. Chen, P. Zhang, H. Wu, Z. Wang, and Z. Zhong, "Prediction of shield tunneling-induced ground settlement using machine learning techniques," *Frontiers of Structural and Civil Engineering*, vol. 13, no. 6, pp. 1363–1378, 2019.
- [23] L. Zhang, X. Chen, Y. Zhang et al., "Application of GWO-ELM model to prediction of caojiatuo landslide displacement in the three gorge reservoir area," *Water*, vol. 12, no. 7, 1860 pages, 2020.
- [24] G.-B. Huang, "An insight into extreme learning machines: random neurons, random features and kernels," *Cognitive Computation*, vol. 6, no. 3, pp. 376–390, 2014.
- [25] G.-B. Huang, Q.-Y. Zhu, and C.-K. Siew, "Extreme learning machine: theory and applications," *Neurocomputing*, vol. 70, no. 1-3, pp. 489–501, 2006.
- [26] J. P. S. Catalao, H. M. I. Pousinho, and V. Mendes, "Hybrid wavelet-PSO-ANFIS approach for short-term wind power forecasting in Portugal," *IEEE Transactions on Sustainable Energy*, vol. 2, no. 3, pp. 50–59, 2010.
- [27] M. Moradi-Jalal and B. W. Karney, "Optimal design and operation of irrigation pumping stations using mathematical programming and genetic algorithm (ga)," *Journal of Hydraulic Research*, vol. 46, no. 2, pp. 237–246, 2008.
- [28] S. Mirjalili, S. M. Mirjalili, and A. Lewis, "Grey wolf optimizer," *Advances in Engineering Software*, vol. 69, no. 3, pp. 46–61, 2014.
- [29] S. Mirjalili, S. Saremi, S. M. Mirjalili, and L. D. S. Coelho, "Multi-objective grey wolf optimizer: a novel algorithm for multi-criterion optimization," *Expert Systems with Applications*, vol. 47, no. 1, pp. 106–119, 2016.
- [30] R. E. Precup, R. C. David, and E. M. Petriu, "Grey wolf optimizer algorithm-based tuning of fuzzy control systems with reduced parametric sensitivity," *IEEE Transactions on Industrial Electronics*, vol. 64, no. 1, pp. 527–534, 2016.
- [31] J. Yu, W. Yao, K. Duan, X. Liu, and Y. Zhu, "Experimental study and discrete element method modeling of compression and permeability behaviors of weakly anisotropic sandstones," *International Journal of Rock Mechanics and Mining Sciences*, vol. 134, Article ID 104437, 2020.
- [32] J. Yu, G. Y. Liu, Y. Y. Cai, J. F. Zhou, S. Y. Liu, and B. X. Tu, "Time-dependent deformation mechanism for swelling soft-rock tunnels in coal mines and its mathematical deduction," *International Journal of Geomechanics*, vol. 20, no. 3, Article ID 04019186, 2020.
- [33] W. Zhou, X. Shi, X. Lu, C. Qi, B. Luan, and F. Liu, "The mechanical and microstructural properties of refuse mudstone-GGBS-red mud based geopolymer composites made with sand," *Construction and Building Materials*, vol. 253, Article ID 119193, 2020.